Journal of Organometallic Chemistry 945 (2021) 121849

Contents lists available at ScienceDirect

Journal of Organometallic Chemistry

journal homepage: www.elsevier.com/locate/jorganchem

Facile synthesis of Pd nanoparticles supported on a novel Schiff base modified chitosan-kaolin: Antibacterial and catalytic activities in Sonogashira coupling reaction

Mahmoud Nasrollahzadeh[a,*], Nasrin Shafiei[a], Talat Baran[b], Khatereh Pakzad[a], Mohammad Reza Tahsili[c], Nuray Yılmaz Baran[d], Mohammadreza Shokouhimehr[e]

[a] Department of Chemistry, Faculty of Science, University of Qom, PO Box 37185-359, Qom, Iran
[b] Department of Chemistry, Faculty of Science and Letters, Aksaray University, 68100 Aksaray, Turkey
[c] Department of Biology, Faculty of Science, University of Qom, PO Box 37185-359, Qom, Iran
[d] Technical Vocational School, Department of Chemistry Technology, Aksaray University, 68100 Aksaray, Turkey
[e] Department of Materials Science and Engineering, Research Institute of Advanced Materials, Seoul National University, Seoul 08826, Republic of Korea

ARTICLE INFO

Article history:
Received 27 November 2020
Revised 17 April 2021
Accepted 20 April 2021
Available online 30 April 2021

Keywords:
SCR
Biopolymer-supported Pd complex
Chitosan

ABSTRACT

The present work studies the Sonogashira coupling reaction (SCR) between aryl halides and acetylenes under aerobic conditions using the catalytic complex of Pd nanoparticles (NPs) supported on a novel Schiff base modified chitosan-kaolin (Pd NPs@CS-Kao) in ethanol solvent. The prepared catalyst was characterized by TEM, SEM, FT-IR, XRD, EDS, XPS, elemental mapping, and Raman analyses. The products were formed in high yields. At the end of the reaction, Pd NPs@CS-Kao can be filtered and reused for five consecutive cycles. The advantages of this catalytic process include simple methodology, high yields, and easy work-up. In addition, Pd NPs@CS-Kao exhibited effective antibacterial performance against *E. coli* gram-negative bacteria.

1. Introduction

One of the most prominent reactions in chemistry is SCR, which is applicable in the preparation of organic compounds, pharmaceuticals and nanomaterials. SCR results in C-C bond formation between terminal alkynes and vinyl or aryl halides and usually employs a Pd catalyst, a Cu(I) co-catalyst, phosphine ligands, an amine base and toxic organic solvents including DMF, benzene, THF, etc., making the process uneconomical and environmentally harmful [1-7].

Palladium catalyzed reactions mostly suffer from drawbacks including long reaction times, harsh conditions, inert atmosphere conditions, tedious work-up, utilization of toxic polar solvents, expensive ligands, environmental pollution due to the production of diyne side product and low yields of the main products, which limit their applications [5,8]. In SCR, copper(I) co-catalyst causes the tansmetallation by the *in situ* production of copper acetylide. Utilization of copper salt may also cause Glaser-type oxidative homocoupling of the terminal acetylene as a by-product [5,8-10]. In addition, amines are environmentally hazardous and foul smelling [11]. Therefore, it is important to investigate novel advantageous conditions for this kind of reaction.

Conventional SCR systems employ homogeneous Pd catalysts. However, heterogeneous catalysts are economical, recyclable, and reusable in several reaction cycles [12-14]. Therefore, the development of heterogeneous Pd catalysts has attracted much attention. Alonso *et al.* prepared a catalyst composed of Pd NPs supported on DNA for copper- and ligand-free Sonogashira-Hagihara coupling of aryl iodides with terminal aromatic and aliphatic alkynes [15].

For the last few decades, biopolymers such as chitosan, chitin, and cellulose have been efficiently applied in the synthesis of heterogeneous catalysts due to their characteristic functional groups [16-21]. The activity, characteristic redox property and high catalytic surface area of biopolymers in chemical transformations can be improved by doping them with metal or metal oxide NPs. Functionalized biopolymers have been extensively studied as heterogeneous catalysts due to their high efficiency, recyclability and ability to perform catalysis.

Among various polymers, chitosan (CS) is of a great importance as it is natural, biodegradable, non-toxic, environmentally benign, positively charged and abundant in the nature. Chitosan is a poly-

---

[*] Corresponding author.
E-mail address: mahmoudnasr81@gmail.com (M. Nasrollahzadeh).

https://doi.org/10.1016/j.jorganchem.2021.121849

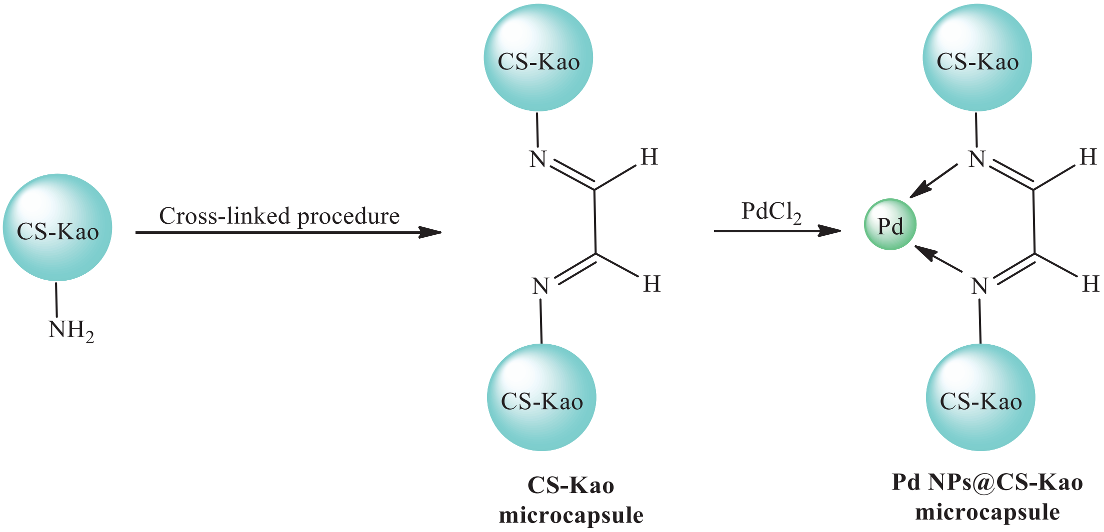

Scheme 1. Schematic representation of the process for the fabrication of Pd NPs@CS-Kao microcapsules.

mer with high tendency for metal adsorption. This polymer can be used as a substrate in the synthesis of heterogeneous catalysts in the form of colloids, fibers or stabilized on inorganic substrates (alumina, silica or other metal oxides). Easy chemical and physical modification of this polymer as well as its environmental compatibility have led to the use of chitosan in a wide range of catalytic reactions. Therefore, it can be a good choice for the preparation of a heterogeneous Pd catalysts [22-27]. In a study, Bahrami and Shahbazi developed palladium metal NPs doped on chitosan nanofibers modified with 2-aminobenzaldehyde as novel heterogeneous catalysts in Heck and Suzuki C-C coupling reactions [28]. Furthermore, Hajipour and Tavangar-Rizi developed Pd NPs immobilized on magnetic methionine functionalized chitosan for utilization in Suzuki and copper-free Sonogashira reactions of aryl halides at room temperature in water [29].

In addition, kaolin is an abundant, natural, negatively charged, low-cost clay consisting of kaolinite and a two layer 1:1 silicate [30,31]. Kaolinite has a two-dimensional and lamellar structure and is abundantly found in highly weathered tropical soils [32,33]. Kaolin is very applicable in different fields. It can be used as pigment and filler in paper industry, extender in water based paints, and additive in polymers. It can also be applied in composites as a reinforcing compound [34].

Our group has published many reports on SCR. In 2009, Pd/Cu system was used to catalyze the reaction of 2-amino-3-(2-propynyl)thiazolium bromide with various iodobenzenes using sodium lauryl sulfate and cesium carbonate as surfactant and base, respectively, in water to form 6-substituted imidazo[2,1-*b*]thiazoles [35]. Later, an effective method was developed using Fe_3O_4@Ni nanoparticles prepared by the extract of the *Euphorbia maculata* for SCR in water in 2020 [36].

Recently, our group has also shown a high interest in polymer supported catalytic systems for different organic reactions including SCR [37]. In 2018, a palladium nanocatalyst stabilized with sustainable chitosan/cellulose composite was synthesized and employed in Suzuki-Miyaura coupling reactions [38]. In addition, a palladium nanocatalyst anchored on magnetic lignin-chitosan beads was prepared for the synthesis of biaryls and aryl halide cyanation [39].

In this work, SCR has been studied using novel Pd NPs supported on a Schiff base modified chitosan-kaolin (Scheme 1) as an effective catalyst under copper- and ligand-free conditions in EtOH solvent. This process is cost effective and environmentally benign.

2. Experimental

2.1. Reagents and instruments

All chemicals were supplied from Sigma Aldrich Chemical Co. and utilized as received. Kaolin was supplied from Turkey. FT-IR spectroscopy using a Perkin Elmer 100 spectrophotometer was performed for characterization of the catalyst and products. EDS analysis of Pd NPs@CS-Kao was carried out using an FEI Quanta 450 FEG instrument. The X-ray and Raman spectra of Pd NPs@CS-Kao were recorded using a Philips model PW 1373 diffractometer (Cu $K\alpha = 1.5406$ Å) and Raman microscope, respectively. The morphology and size of the nanocatalyst were investigated by TEM (JEM-F200 JEOL) technique. XPS was carried out using an Al $K\alpha$ source (PHI 5000 VersaProbe).

2.2. Preparation of CS-Kao microcapsules

Following the reaction sequence outlined in Scheme 1, chitosan (2 g) was dissolved in 100 mL of 2% acetic acid solution (v:v) and the resulting solution was treated with kaolin (2 g) under stirring at ambient temperature. After 3 h, the reaction mixture was poured into an alkaline solution (water: methanol: NaOH, 40 mL: 60 mL: 12 g) to form gelatinous microspheres. The synthesized chitosan-kaolin microspheres were extensively washed with water to neutrality and then treated with glyoxal solution (5 mL) in methanol (50 mL). The mixture obtained was stirred for a day under reflux conditions for cross-linking. Finally, CS-Kao microspheres were filtered, washed with methanol and dried (Scheme 2).

2.3. Preparation of Pd NPs on CS-Kao microspheres

A mixture of CS-Kao microcapsules (1 g) and $PdCl_2$ (0.2 g) in 30 mL of ethanol was heated to 70 °C under stirring for 3 h. The reaction mixture was then cooled and the Pd NPs loaded on the CS-Kao microcapsules were filtered, washed with EtOH and dried.

2.4. General process for SCR

The reaction between an aryl halide (1 mmol) and a terminal alkyne (1.1 mmol) was carried out using Pd NPs@CS-Kao (40 mg) and K_2CO_3 (1.5 mmol) in ethanol solvent (8 mL) under reflux conditions at 80 °C for the proper times. The progress of the reaction was followed by TLC. At the end of the reaction, the mixture was

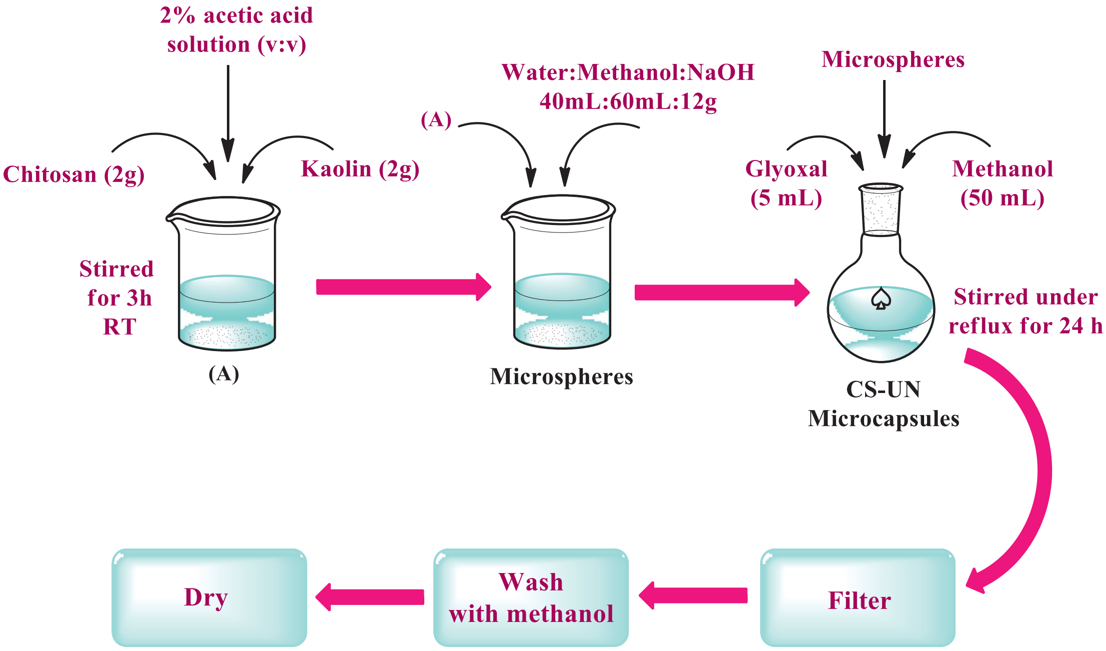

Scheme 2. Schematic representation of the process for the organization of CS-Kao microcapsules.

cooled, the catalyst was filtered, and the solvent was evaporated. The as-prepared residue was purified with n-hexane and acetone to obtain the pure product. All the products obtained were known compounds and their spectral data matched the literature values.

2.5. Characterization data of selected products

1-Nitro-4-(phenylethynyl)benzene
^{1}HNMR (400 MHz, $CDCl_3$) $\delta_H = 8.25$ (d, $J = 9.0$ Hz, 2H), 7.69 (d, $J = 9.0$ Hz, 2H), 7.59-7.56 (m, 2H), 7.43-7.39 (m, 3H); ^{13}CNMR (100 MHz, $CDCl_3$) δ_C = 132.3, 131.8, 130.4, 129.3, 128.5, 123.6, 122.1, 115.6, 94.9, 87.4.

4-(Phenylethynyl)benzonitrile
^{1}HNMR (400 MHz, $CDCl_3$) $\delta_H = 8.30$ (d, $J = 8.6$ Hz, 2H), 8.07 (d, $J = 8.6$ Hz, 2H), 7.94-7.91 (m, 2H), 7.54-7.51 (m, 3H).

1-Methyl-4-(oct-1-yn-1-yl)benzene
^{1}HNMR (400 MHz, $CDCl_3$) $\delta_H = 7.31$ (d, $J = 7.8$ Hz, 2H), 7.10 (d, $J = 7.8$ Hz, 2H), 2.41 (t, $J = 7.2$ Hz, 2H), 2.35 (s, 3H), 1.65-1.43 (m, 8H), 0.94 (s, 3H).

2.6. Antibacterial activity for Pd NPs@CS-Kao

To assess the Pd NPs@CS-Kao antibacterial efficiency, *E. coli* (ATCC: 35218) was cultured by Difco^{TM} nutrient agar medium. The potential antibacterial activity of Pd NPs@CS-Kao was monitored by the disk diffusion method. The ~10^6 *Cfu* (Colony-forming unit) mL^{-1} concentration was immunized on nutrient agar plates. A filter paper with a diameter of 0.4 cm diameter was immersed in 10, 20, and 35 μg mL^{-1} of the constituent and then dispersed on the surface of bacteria inoculated agar plates. After 12 h incubation at 37.5°C, the inhibition zone was measured.

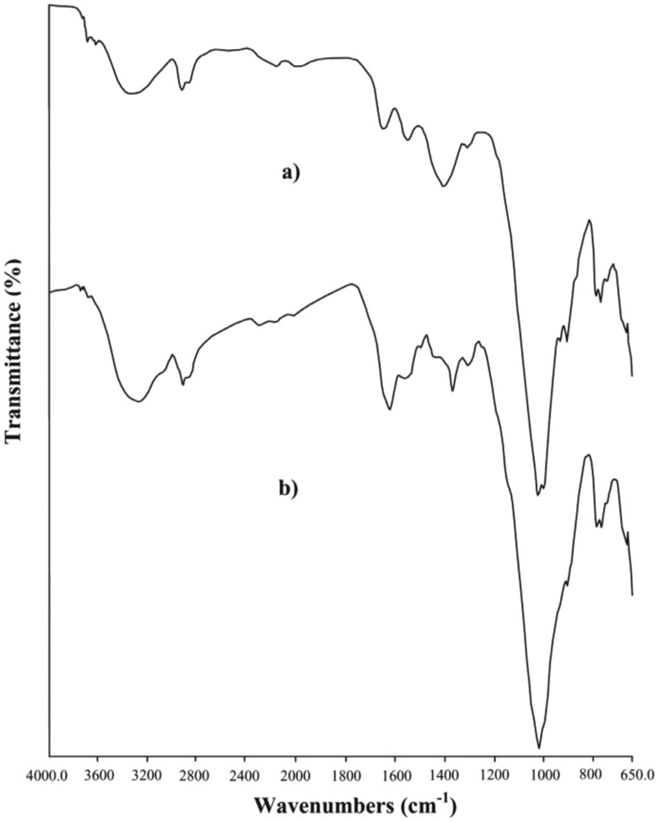

Fig. 1. FT-IR spectra of a) CS-Kao and b) Pd NPs@CS-Kao.

3. Results and discussion

3.1. Pd NPs@CS-Kao characterization

Fig. 1 represents the FTIR spectra of CS-Kao and Pd NPs@CS-Kao. The bands at approximately 3352, 2930 and 2870 cm^{-1} correspond to the O-H and C-H stretching vibrations, respectively. The band at 1027 cm^{-1} is ascribed to the C-O-C stretching vibration. Additionally, the band at 1645 cm^{-1} is due to the stretching vibration modes of the imine, confirming the formation of Cs-Kao microcapsule. As for Pd NPs@CS-Kao microspheres, the band corresponding to imine shifted to 1628 cm^{-1} due to the strong interaction of Pd with CS-Kao microcapsule (Fig. 1).

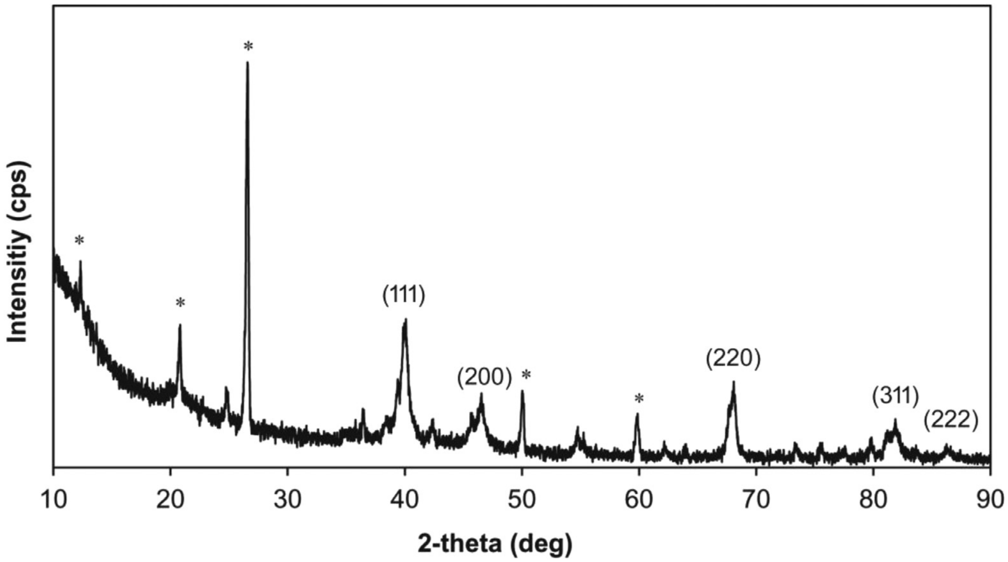

Fig. 2. XRD spectrum of the Pd NPs@CS-Kao.

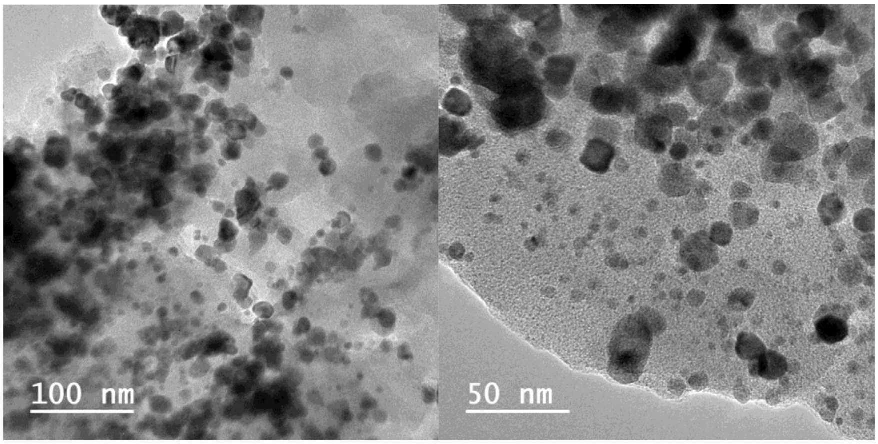

Fig. 3. TEM analysis of Pd NPs@CS-Kao.

Fig. 2 shows the XRD spectrum of Pd NPs@CS-Kao catalyst. All the characteristic peaks of natural kaolin and chitosan are observed in the spectrum. The XRD spectrum of the catalyst displays characteristic peaks at 12.30° and 26.58° (kaolinite minerals), 20.83° (chlorite mineral and chitosan peak), and 50.08° and 59.86° (quartz) [40-42]. Other than the peaks corresponding to kaolin and chitosan, new significant peaks are observed at 40.09° (111), 46.55° (200), 68.08° (220), 81.88° (311) and 86.12° (222) in the XRD spectrum of Pd NPs@CS-Kao corresponding to the face centered cubic (*FCC*) structure of Pd [43], confirming the organization of Pd NPs on the CS-Kao microcapsules.

To verify the formation of Pd NPs, TEM analysis of Pd NPs@CS-Kao catalyst was performed below 100 nm. Pd NPs are clearly observed as black dots in Fig. 3. These results confirm that Pd NPs have been successfully loaded on the designed CS-Kao microcapsules. Additionally, the images show that Pd NPs has spherical morphologies with an average size of about 15-20 nm. Since the average size of the microcapsules varies in the range of 800-1000 µm, they cannot be observed by TEM analysis. To confirm the formation of microcapsules, the SEM analysis of CS-Kao and Pd NPs@CS-Kao catalyst was carried out (Fig. 4). These images indicate that CS-Kao and Pd NPs@CS-Kao are spherically shaped.

EDS analysis gives evidence for the decoration of Pd NPs on the designed CS-Kao microcapsules (Fig. 5).

Raman spectroscopy was also used for the characterization of Pd NPs@CS-Kao, as shown in Fig. 6. According to the Raman spectrum of pure chitosan in the literature [44], the Raman spectrum of Pd NPs@CS-Kao catalyst shows changes compared to chitosan, which confirms the fabrication of the catalyst.

Elemental mapping analysis of catalyst was also carried out to verify the formation of Pd NPs (Fig. 7). This analysis shows that Pd NPs have been successfully decorated on the support surface.

The XPS analysis of Pd NPs@CS-Kao was also performed to ascertain the formation of Pd NPs (Fig. 8), illustrating the presence of two chemical states of Pd. The lower binding energy of Pd can be assigned to the metallic Pd; while the higher binding energy demonstrates PdO due to the surface partial oxidation of Pd NPs [45-48].

3.2. Catalytic prowess of Pd NPs@CS-Kao in the SCR

This study introduces Pd NPs@CS-Kao as a Schiff base modified catalyst for SCR under ligand-, copper- and phosphine-free conditions.

In this study, the reaction conditions were optimized considering several solvents and bases as well as catalyst amounts in the reaction of 1.0 mmol of *p*-iodoanisole with 1.1 mmol of phenylacetylene using Pd NPs@CS-Kao catalyst, 8.0 mL of solvent and

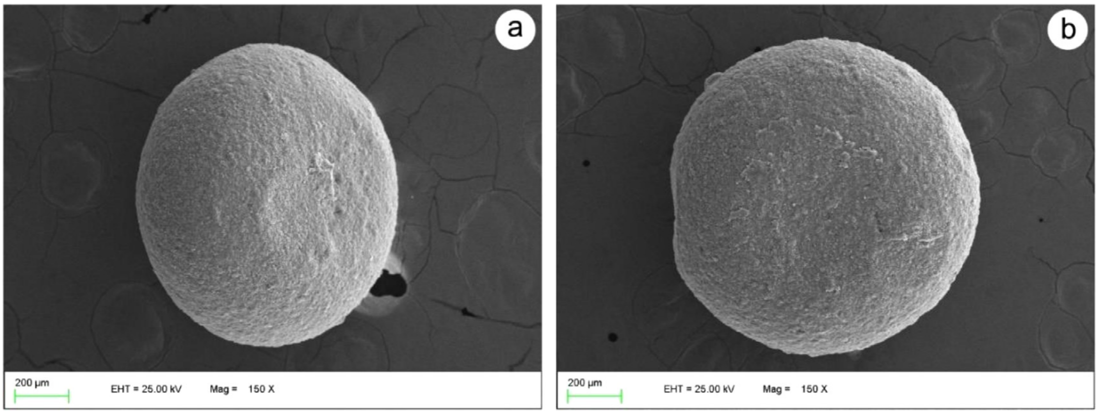

Fig. 4. SEM images of a) CS-Kao and b) Pd NPs@CS-Kao microcapsule.

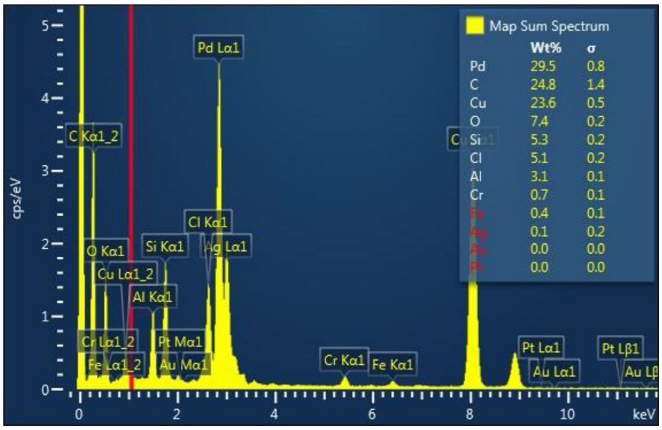

Fig. 5. EDS analysis of Pd NPs@CS-Kao.

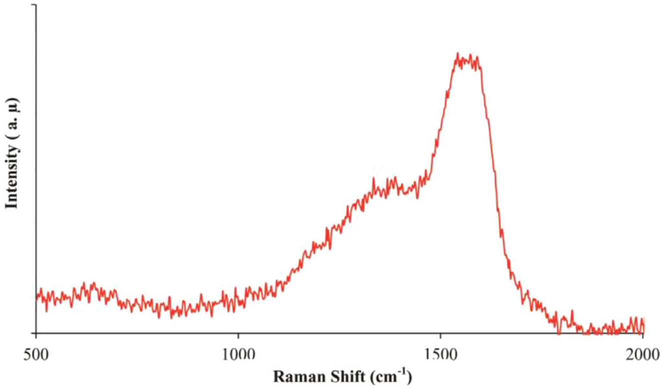

Fig. 6. Raman spectrum of Pd NPs@CS-Kao.

1.5 mmol of base as the model reaction. Firstly, SCR was carried out without any catalyst at 80 °C (Table 1, entry 1), which yielded no product. As shown in Table 1, the choice of solvent or base somewhat influences the reaction. The efficacy of Pd NPs@CS-Kao catalyst (40 mg) was estimated in the presence of different bases (K_2CO_3, pyridine, KOH, NEt_3, NaOH, and Na_2CO_3) and solvents (toluene, H_2O, EtOH, and H_2O/EtOH). The best results were obtained in the presence of K_2CO_3, ethanol and 40 mg of catalysts for 3 h at 80 °C (Table 1, entry 10). Concerning the above results, the effect of the amount of Pd NPs@CS-Kao catalyst was examined. According to the results, upon decreasing the quantity of the catalyst from 40 to 20 mg, the product yield decreases from 85 to 53%. However, increasing the amount of catalyst from 40 to 50 mg slightly increases the product yield from 85 to 86%.

Table 1
Optimization of SCR conditions in the reaction of phenylacetylene with *p*-iodoanisole at 80 °C for 3 h.

Entry	Pd NPs@CS-Kao (mg)	Solvent	Base	Yield (%)
1	None	EtOH	K_2CO_3	0
2	40	H_2O	K_2CO_3	Trace
3	40	Toluene	K_2CO_3	41
4	40	H_2O/EtOH	K_2CO_3	17
5	40	EtOH	Pyridine	34
6	40	EtOH	KOH	55
7	40	EtOH	NEt_3	59
8	40	EtOH	NaOH	40
9	40	EtOH	Na_2CO_3	76
10	40	EtOH	K_2CO_3	85
11	20	EtOH	K_2CO_3	53
12	50	EtOH	K_2CO_3	86

Next, the application of Pd NPs@CS-Kao was investigated in the SCR between terminal acetylenes and different aryl halides containing both electron withdrawing and donating groups under the optimized conditions. According to Table 2, it is clear that the system is practically applicable for various aryl halides. Good to excellent product yields are obtained in all cases under the reaction conditions. In addition, chlorobenzene effectively forms the corresponding product in 68% yield (Table 2, entry 11).

According to the literature [3,37,49,50], the plausible mechanism for SCR is shown in Scheme 3. The first step involves the activation of the phenylacetylene terminal acetylene C-H with Pd NPs@CS-Kao. Subsequently, potassium acetylide intermediate is formed *via* C-H deprotonation with K_2CO_3. Aryl palladium halide complex (ArPdX) can be produced *via* activation of ArX on the Pd NPs@CS-Kao sites. Finally, reductive elimination causes the production of the desired coupling product.

The melting points of all the products match those of authentic samples [51-53]. The NMR spectra also confirm the structure of the products (See Supporting Information).

3.3. Catalyst recyclability

One of the vital properties of catalysts is their recyclability [54,55]. In this study, the recyclability of Pd NPs@CS-Kao cata-

Table 2
Pd NPs@CS-Kao catalyzed SCR of terminal alkynes with different aryl halides.[a]

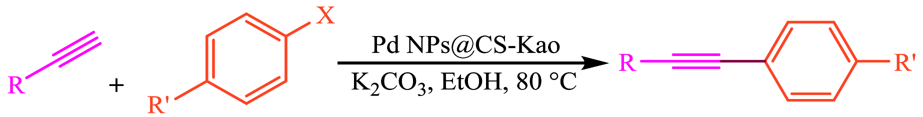

X = I, Cl & Br

Entry	R	Aryl halide	Product	Time (h)	Yield (%)[b]
1	Ph	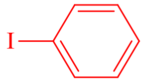	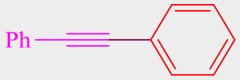	3	88
2	Ph	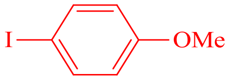	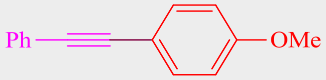	3	85
3	Ph	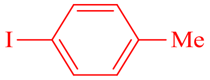	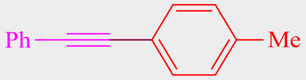	3	85
4	Ph	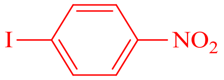	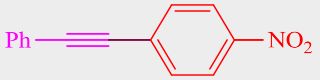	2.5	89
5	Ph	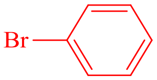	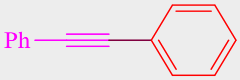	5	78
6	Ph	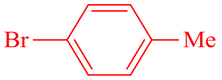	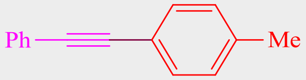	5	72
7	Ph	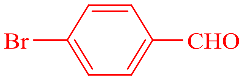	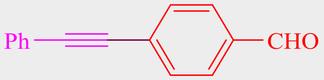	6	70
8	Ph	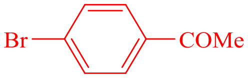	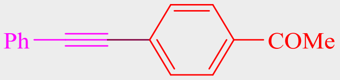	6	69
9	Ph	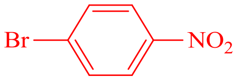	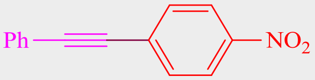	5	77
10	Ph	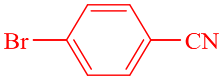	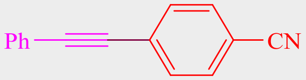	5	76
11	Ph	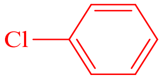	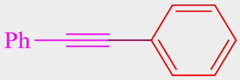	7	68
12	Me-$(CH_2)_5$-	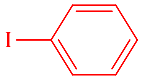	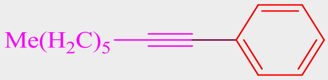	8	80
13	Me-$(CH_2)_5$-	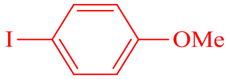	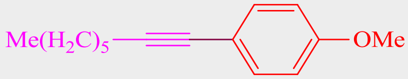	8	77
14	Me-$(CH_2)_5$-	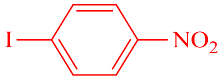	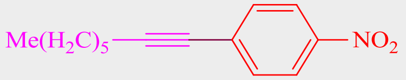	8	82
15	Me-$(CH_2)_5$-	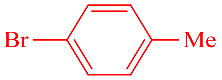	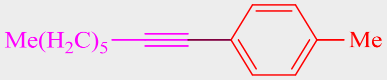	8	72

---

[a] Reaction conditions: Terminal acetylene (1.1 mmol), aryl halide (1 mmol), K_2CO_3 (1.5 mmol), catalyst (40 mg), EtOH (8 mL), 80 °C.
[b] Isolated yield.

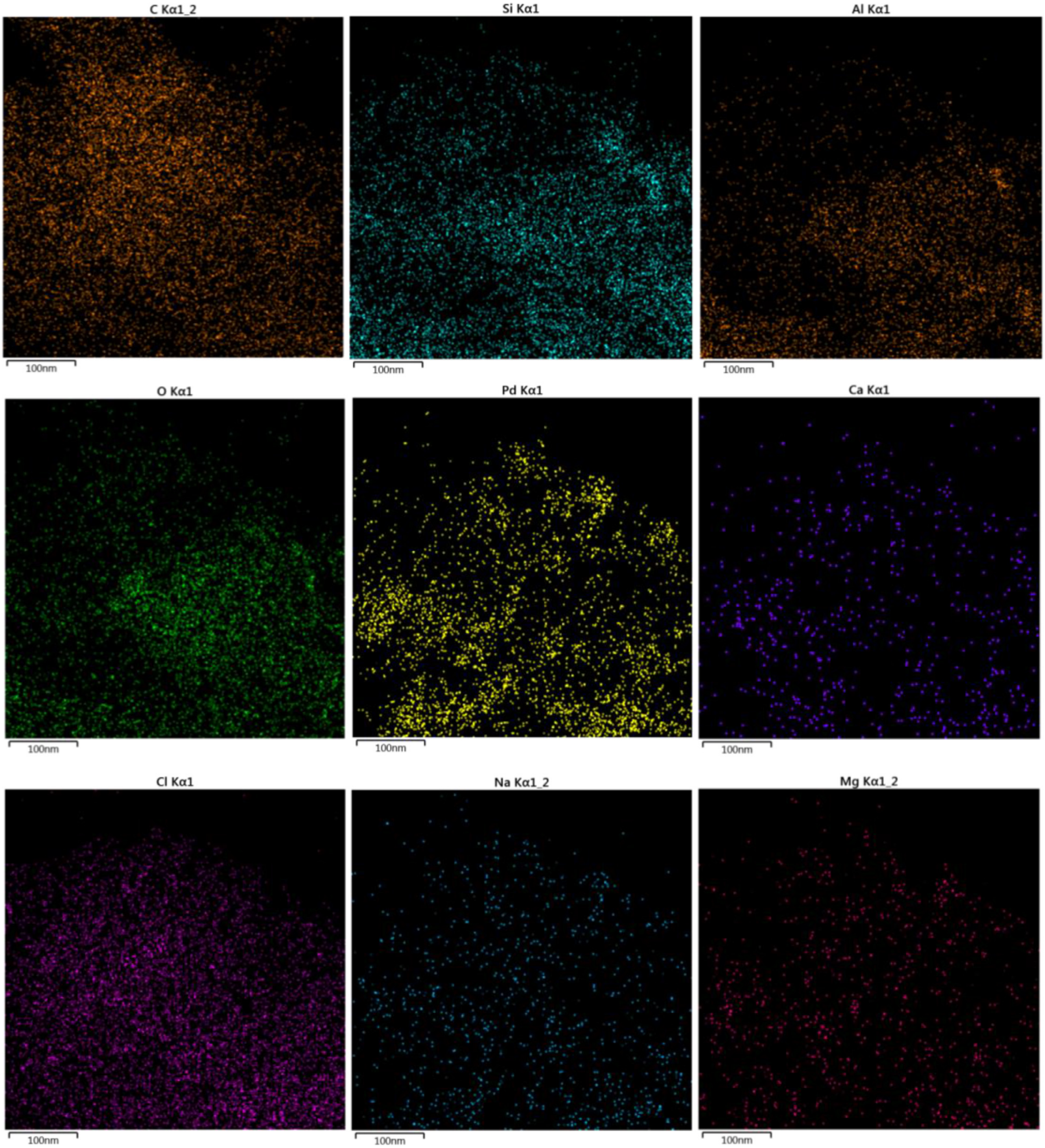

Fig. 7. Elemental mapping analysis of Pd NPs@CS-Kao.

lyst was evaluated in the SCR reaction of phenylacetylene and 4-iodotoluene under optimal reaction conditions. After completion of SCR, the catalyst was separated by filtration, washed with EtOAc, dried at 100 °C in a hot air oven for 4 h, and reused in the next cycle. The catalyst was found to be recyclable with high catalytic activity for up to five consecutive cycles. As shown in Fig. 9, the catalytic activity of Pd NPs@CS-Kao decreases slightly in the fifth cycle.

3.4. Antibacterial activity of Pd NPs@CS-Kao

The antibacterial prowess of Pd NPs@CS-Kao was monitored by the disk diffusion method. As shown in Fig. 10, Pd NPs@CS-Kao was shown to possess effective antibacterial activity against *E. coli* (gram-negative) bacteria. The diameter of the antibacterial region formed by the antibacterial Pd NPs @ CS-Kao was measured in millimeters from the closest point to the center, as shown in Table 3. As shown in Fig. 10, Pd NPs@CS-Kao shows good antibac-

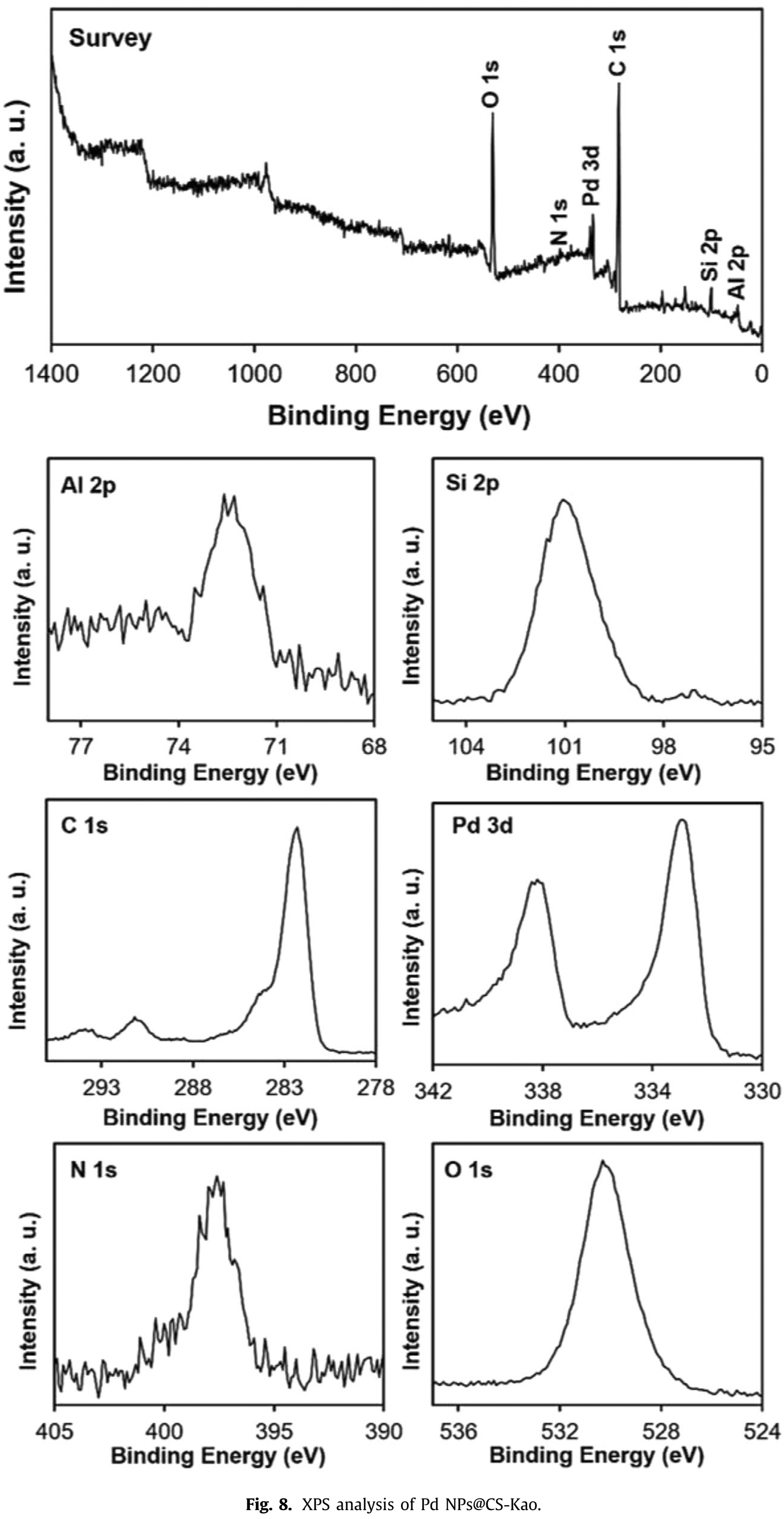

Fig. 8. XPS analysis of Pd NPs@CS-Kao.

Table 3
Antibacterial efficiency of Pd NPs@CS-Kao against *E. coli*.

Entry	Symbol	Pd NPs@CS-Kao (μg mL^{-1})	Inhibition zone (mm)	Result
1	a	35	19.5	Resistance
2	b	20	10.5	Intermediate
3	c	10	6	Susceptible

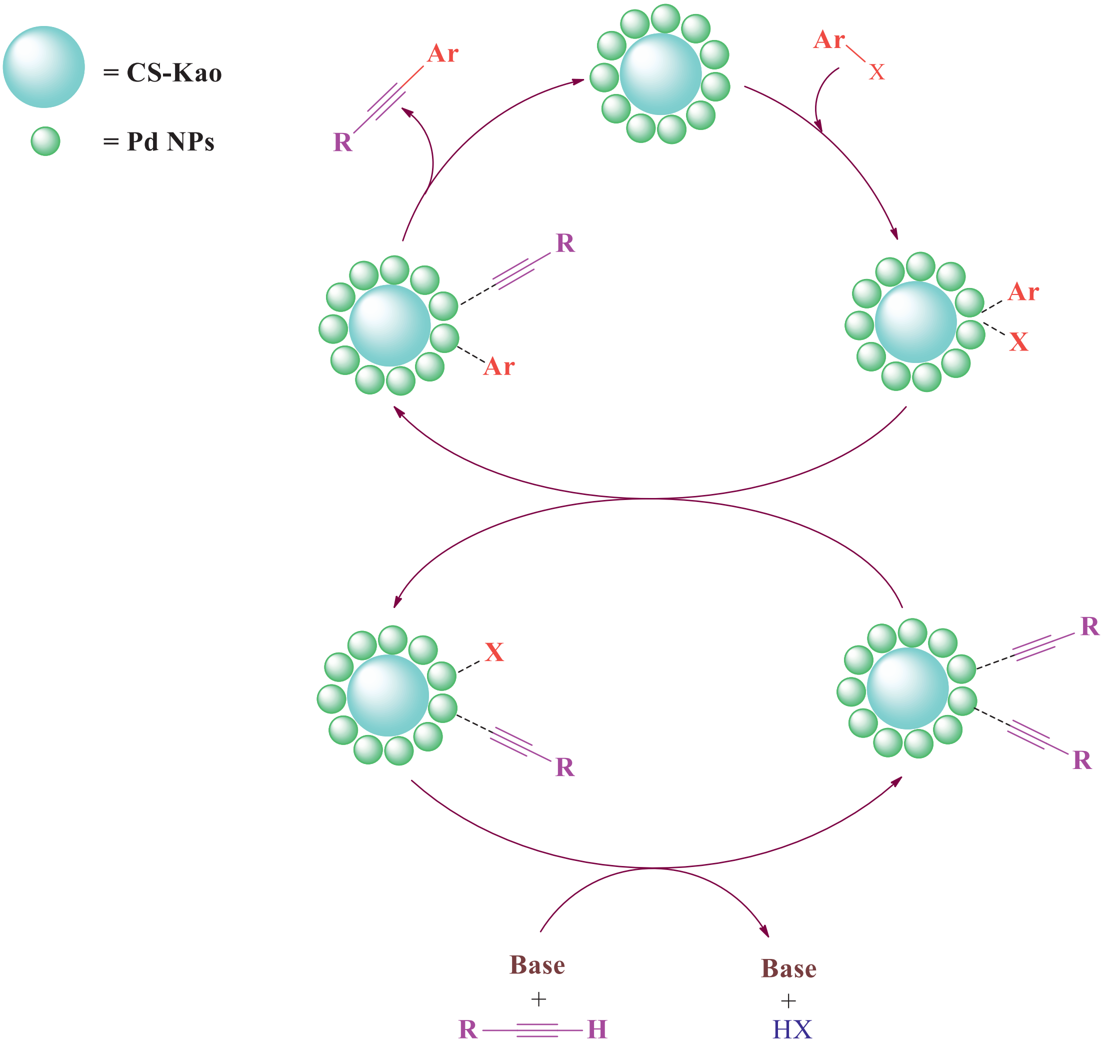

Scheme 3. Proposed mechanism for SCR using Pd NPs@CS-Kao catalyst.

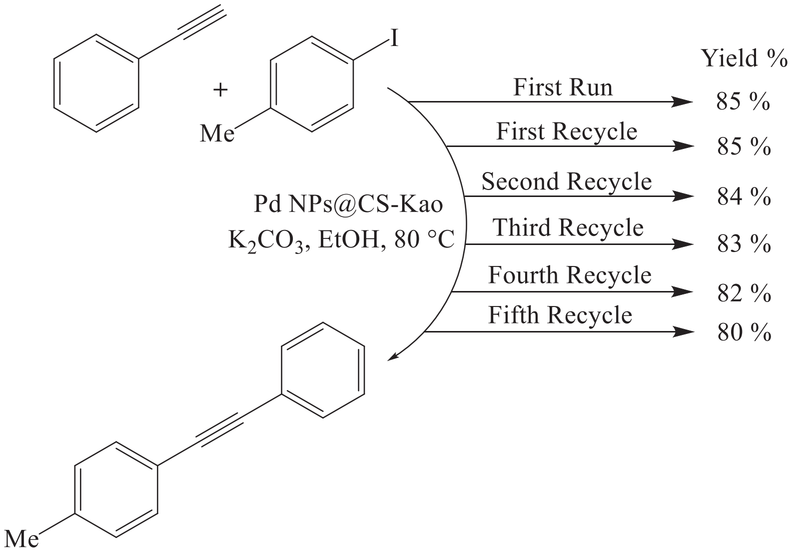

Fig. 9. Reusability of Pd NPs@CS-Kao in SCR.

Fig. 10. Disk diffusion used to determine the antibacterial efficiency of Pd NPs@CS-Kao on *E. coli*.

terial prowess against *E. coli*. Of the three different constructions of NPs@CS-Kao, only 35 μg mL^{-1} is susceptible by the disk diffusion method.

4. Conclusion

In summary, Pd NPs@CS-Kao has been designed as an environmentally benign catalyst using chitosan and kaolin as natural compounds and its efficacy has been studied in SCR. FT-IR, XRD, EDS, SEM, XPS, Raman, elemental mapping and TEM analyses were applied to characterize this Schiff base modified heterogeneous catalyst. These characterization methods proved the catalyst formation and the presence of Pd NPs with particle size of about 15-20 nm. The designed catalyst showed high efficacy, stability and recyclability for five consecutive runs in SCR. A variety of starting materials were used to obtain products in high yields. The low cost, simplicity of separation and outstanding reusability are some advantages of this catalyst, which make it even more appealing for catalytic applications in different organic reactions. Furthermore, Pd NPs@CS-Kao showed excellent antibacterial performance against *E. coli* gram-negative bacteria.

Declaration of Competing Interest

The authors declare that they have no known competing financial interests or personal relationships that could have appeared to influence the work reported in this paper.

Acknowledgments

We gratefully acknowledge the University of Qom for the support of this work.

Supplementary materials

Supplementary material associated with this article can be found, in the online version, at doi:10.1016/j.jorganchem.2021.121849.

References

[1] A.R. Gholap, K. Venkatesan, R. Pasricha, T. Daniel, R.J. Lahoti, K.V. Srinivasan, Copper- and ligand-free Sonogashira reaction catalyzed by Pd(0) nanoparticles at ambient conditions under ultrasound irradiation, J. Org. Chem. 70 (2005) 4869–4872.
[2] X.F. Wu, H. Neumann, M. Beller, Palladium-catalyzed carbonylative coupling reactions between Ar–X and carbon nucleophiles, Chem. Soc. Rev. 40 (2011) 4986–5009.
[3] R. Chinchilla, C. Nájera, Recent advances in Sonogashira reactions, Chem. Soc. Rev. 40 (2011) 5084–5121.
[4] E. Negishi, L. Anastasia, Palladium-catalyzed alkynylation, Chem. Rev. 103 (2003) 1979–2018.
[5] H. Doucet, J.C. Hierso, Palladium-based catalytic systems for the synthesis of conjugated enynes by Sonogashira reactions and related alkynylations, Angew. Chem. Int. Ed. 46 (2007) 834–871.
[6] K. Sonogashira, Development of Pd–Cu catalyzed cross-coupling of terminal acetylenes with sp^2-carbon halides, J. Organomet. Chem. 653 (2002) 46–49.
[7] M. Nasrollahzadeh, Z. Issaabadi, M.M. Tohidi, S.M. Sajadi, Recent progress in application of graphene supported metal nanoparticles in C-C and C-X coupling reactions, Chem. Rec. 18 (2) (2018) 165–229.
[8] K. Sonogashira, Comprehensive organic synthesis, Pergamon: New York, 3 (1991) 521.
[9] A. Sagadevan, K.C. Hwang, Photo-induced Sonogashira C–C coupling reaction catalyzed by simple copper(I) chloride salt at room temperature, Adv. Synth. Catal. 354 (2012) 3421–3427.
[10] Y. Yamane, N. Miwa, T. Nishikata, Copper-catalyzed functionalized tertiary-alkylative Sonogashira type couplings via copper acetylide at room temperature, ACS Catal 7 (2017) 6872–6876.
[11] W.N. Albrecht, R.L. Stephenson, Health hazards of tertiary amine catalysts, Scand. J. Work Environ. Health 14 (1988) 209–219.
[12] A. Molnar, Efficient, selective, and recyclable palladium catalysts in carbon-carbon coupling reactions, Chem. Rev. 111 (2011) 2251–2320.
[13] M. Lamblin, L. Nassar-Hardy, J. Hierso, E. Fouquet, F. Felpin, Recyclable heterogeneous palladium catalysts in pure water: Sustainable developments in Suzuki, Heck, Sonogashira and Tsuji–Trost reactions, Adv. Synth. Catal. 352 (2010) 33–79.
[14] M. Gholinejad, N. Jeddi, B. Pullithadathil, Agarose functionalized phosphorus ligand for stabilization of small-sized palladium and copper nanoparticles: efficient heterogeneous catalyst for Sonogashira reaction, Tetrahedron 72 (2016) 2491–2500.
[15] A.S. Camacho, I. Martin-Garcia, C. Contreras-Celedon, L. Chacon-Garcia, F. Alonso, DNA-supported palladium nanoparticles as a reusable catalyst for the copper-and ligand-free Sonogashira reaction, Catal. Sci. Tech. 7 (2017) 2262–2273.
[16] Q. Liu, J. Li, Y. Zhao, Y. Zhou, C. Li, CdS nanoparticle-functionalized natural cotton cellulose electrospun nanofibers for visible light photocatalysis, Mater. Lett. 138 (2015) 89–91.
[17] A. Fakhri, V.K. Gupta, H. Rabizadeh, S. Agarwal, N. Sadeghi, S. Tahami, Preparation and characterization of WS$_2$ decorated and immobilized on chitosan and polycaprolactone as biodegradable polymers nanofibers: Photocatalysis study and antibiotic-conjugated for antibacterial evaluation, Int. J. Biol. Macromol. 120 (2018) 1789–1793.
[18] S. Bano, N. Ahmad, S. Sultana, S. Sabir, M.Z. Khan, Preparation and Study of Ternary Polypyrrole-Tin oxide-Chitin nanocomposites and their potential applications in visible light photocatalysis and sensors, J. Environ. Chem. Eng. 7 (2) (2019) 103012.
[19] S. Sultana, N. Ahmad, S.M. Faisal, M. Owais, S. Sabir, Synthesis, characterization and potential applications of polyaniline/chitosan-Ag-nano-biocomposite, IET Nanobiotechnol. 11 (7) (2017) 835–842.
[20] G. Crini, P.M. Badot, Application of chitosan, a natural amino polysaccharide, for dye removal from aqueous solutions by adsorption processes using batch studies: a review of recent literature, Prog. Polym. Sci. 33 (4) (2008) 399–447.
[21] G. Copello, J.A.M. Mebert, M. Raineri, M.P. Pesenti, L.E. Diaz, Removal of dyes from water using chitosan hydrogel/SiO$_2$ and chitin hydrogel/SiO$_2$ hybrid materials obtained by the sol-gel method, J. Hazard. Mater. 186 (1) (2011) 932–939.
[22] A. Kumbhar, R. Salunkhe, Recent advances in biopolymer supported palladium in organic synthesis, Curr. Org. Chem. 19 (2015) 2075–2121.
[23] P. Cotugno, M. Casiello, A. Nacci, P. Mastrorilli, M.M. Dell'Anna, A. Monopoli, Suzuki coupling of iodo and bromoarenes catalyzed by chitosan-supported Pd–nanoparticles in ionic liquids, J. Organomet. Chem. 752 (2014) 1–5.
[24] K. Khalil, H. Al-Matar, Chitosan based heterogeneous catalyses: Chitosan–grafted-poly(4-vinylpyridne) as an efficient catalyst for michael additions and alkylpyridazinyl carbonitrile oxidation, Molecules 18 (2013) 5288–5305.
[25] M. Lee, B.-Y. Chen, W. Den, Chitosan as a natural polymer for heterogeneous catalysts support: a short review on its applications, Appl. Sci. 5 (2015) 1272–1283.
[26] D.J. Macquarrie, J.J.E. Hardy, Applications of functionalized chitosan in catalysis, Ind. Eng. Chem. Res. 44 (2005) 8499–8520.
[27] S.E. Leonhardt, A. Stolle, B. Ondruschka, G. Cravotto, C. De Leo, K.D. Jandt, T.F. Keller, Chitosan as a support for heterogeneous Pd catalysts in liquid phase catalysis, Appl. Catal. A-Gen. 379 (2010) 30–37.
[28] E. Shahbazi, K. Bahrami, Palladium nanoparticles doped on the chitosan nanofibers modified with 2-aminobenzaldehyde as a nanocatalyst in cross–coupling reactions, ChemistrySelect 5 (2020) 5489–5496.

[29] A.R. Hajipour, Z. Tavangar-Rizi Palladium nanoparticles immobilized on magnetic methionine-functionalized chitosan: A versatile catalyst for Suzuki and copper-free Sonogashira reactions of aryl halides at room temperature in water as only solvent, Appl. Organomet. Chem. 31 (2017) e3701.

[30] Y.G. Abou El-Reash, M. Otto, I.M. Kenawy, A.M. Ouf, Adsorption of Cr(VI) and As(V) ions by modified magnetic chitosan chelating resin, Int. J. Biol. Macromol. 49 (2011) 513–522.

[31] H.-Y. Zhu, R. Jiang, L. Xiao, Adsorption of an anionic azo dye by chitosan/kaolin/γ-Fe_2O_3 composites, Appl. Clay Sci. 48 (2010) 522–526.

[32] S. Nakagaki, F.L. Benedito, F. Wypych, Anionic iron(III) porphyrin immobilized on silanized kaolinite as catalyst for oxidation reactions, J. Mol. Catal. A Chem. 217 (2004) 121–131.

[33] P. Srivastava, B. Singh, M. Angove, Competitive adsorption behavior of heavy metals on kaolinite, J. Colloid Interface Sci. 290 (2005) 28–38.

[34] H. Ismail, W.S. Khoo, A. Ariffin, Effects of halloysite nanotubes and kaolin loading on the tensile, swelling, and oxidative degradation properties of poly (vinyl alcohol)/chitosan blends, J. Vinyl Addit. Technol. 19 (2013) 55–64.

[35] T.A. Kamali, M. Bakherad, D. Habibi, S. Farhangi, M. Nasrollahzadeh, Synthesis of 6-substituted imidazo[2,1-*b*]thiazoles via Pd/Cu-mediated Sonogashira coupling in water, Tetrahedron Lett 50 (2009) 5459–5462.

[36] H. Alinezhad, K. Pakzad, M. Nasrollahzadeh, Efficient Sonogashira and A^3 coupling reactions catalyzed by biosynthesized magnetic Fe_3O_4@Ni nanoparticles from *Euphorbia maculata* extract, Appl. Organomet. Chem. 34 (4) (2020) e5473.

[37] M. Nasrollahzadeh, N. Motahharifar, F. Ghorbannezhad, N.S.S. Bidgoli, T. Baran, R.S. Varma, Recent advances in polymer supported palladium complexes as (nano)catalysts for Sonogashira coupling reaction, Mol. Catal. 480 (2020) 110645.

[38] N. Yılmaz Baran, T. Baran, A. Menteş, Production of novel palladium nanocatalyst stabilized with sustainable chitosan/cellulose composite and its catalytic performance in Suzuki-Miyaura coupling reactions, Carbohydr. Polym. 181 (2018) 596–604.

[39] T. Baran, I. Sargin, Green synthesis of a palladium nanocatalyst anchored on magnetic lignin-chitosan beads for synthesis of biaryls and aryl halide cyanation, Int. J. Biol. Macromol. 155 (2020) 814–822.

[40] R. Dewi, H. Agusnar, Z. Alfian, Tamrin, Characterization of technical kaolin using XRF, SEM, XRD, FTIR and its potentials as industrial raw materials, IOP Conf. Ser. J. Phys. Conf. Ser. 1116 (2018) 042010.

[41] A.H. Zyoud, A. Zubi, S.H. Zyoud, M.H. Hilal, S. Zyoud, N. Qamhieh, A. Hajamohideen, H.S. Hilal, Kaolin-supported ZnO nanoparticle catalysts in self-sensitized tetracycline photodegradation: Zero-point charge and pH effects, Appl. Clay Sci. 182 (2019) 105294.

[42] B. Ilić, V. Radonjanin, M. Malešev, M. Zdujić, A. Mitrović, Effects of mechanical and thermal activation on pozzolanic activity of kaolin containing mica, Appl. Clay Sci. 123 (2016) 173–181.

[43] M. Khan, M. Khan, M. Kuniyil, S.F. Adil, A. Al-Warthan, H.Z. Alkhathlan, W. Tremel, M.N. Tahir, M.R.H. Siddiqui, Biogenic synthesis of palladium nanoparticles using *Pulicaria glutinosa* extract and their catalytic activity towards the Suzuki coupling reaction, Dalton Trans 43 (2014) 9026–9031.

[44] X.D. Ren, Q.S. Liu, H. Feng, X.Y. Yin, The characterization of chitosan nanoparticles by Raman spectroscopy, Appl. Mech. Mater. 665 (2014) 367–370.

[45] M. Shokouhimehr, T. Kim, S.W. Jun, K. Shin, Y. Jang, B.H. Kim, J. Kim, T. Hyeon, Magnetically separable carbon nanocomposite catalysts for efficient nitroarene reduction and Suzuki reactions, Appl. Catal. A Gen. 476 (2014) 133–139.

[46] L.J. Wang, J. Zhang, X. Zhao, L.L. Xu, Z.Y. Lyu, M. Lai, W. Chen, Palladium nanoparticle functionalized graphene nanosheets for Li-O_2 batteries: enhanced performance by tailoring the morphology of the discharge product, RSC Adv 5 (2015) 73451–73456.

[47] X. Zhao, J. Zhu, L. Liang, C. Liu, J. Liao, W. Xing, Enhanced electroactivity of Pd nanocrystals supported on $H_3PMo_{12}O_{40}$/carbon for formic acid electrooxidation, J. Power Sources 210 (2012) 392–396.

[48] B. van Devener, S.L. Anderson, T. Shimizu, H. Wang, J. Nabity, J. Engel, J. Yu, D. Wickham, S. Williams, In Situ generation of Pd/PdO nanoparticle methane combustion catalyst: correlation of particle surface chemistry with ignition, J. Phys. Chem. C 113 (2009) 20632–20639.

[49] M. Gazvoda, M. Virant, B. Pinter, J. Košmrlj, Mechanism of copper-free Sonogashira reaction operates through palladium-palladium transmetallation, Nat. Commun. 9 (2018) 1–9.

[50] M. G. Melchor, The Cu-Free Sonogashira Reaction Mechanism. In: A theoretical Study of Pd-Catalyzed C-C Cross-Coupling Reactions. Springer Theses (Recognizing Outstanding Ph.D. Research). Springer, Cham. (2013).

[51] Y. Yang, J.F.Y. Lim, X.-Y. Chew, E.G. Robins, C.W. Johannes, Y.H. Lim, H. Jong, Palladium precatalysts containing *meta*-terarylphosphine ligands for expedient copper-free Sonogashira cross-coupling reactions, Catal. Sci. Technol. 5 (2015) 3501–3506.

[52] A. Sagadevan, K.C. Hwang, Photo-induced Sonogashira C-C coupling reaction catalyzed by simple copper(I) chloride salt at room temperature, Adv. Synth. Catal. 354 (2012) 3421–3427.

[53] Y. Yang, Y.H. Lim, E.G. Robins, C.W. Johannes, Decarboxylative/Sonogashira-type cross-coupling using $PdCl_2(Cy^*Phine)_2$, RSC Adv 6 (2016) 72810–72814.

[54] M. Nasrollahzadeh, M. Sajjadi, M. Maham, S.M. Sajadi, A.A. Barzinjy, Preparation of Pd/Fe_3O_4 nanoparticles by use of *Euphorbia stracheyi Boiss* root extract: A magnetically recoverable catalyst for one-pot reductive amination of aldehydes at room temperature, J. Colloid Interface Sci. 464 (2016) 147–152.

[55] T. Baran, İ. Sargın, M. Kaya, P. Mulerčikas, S. Kazlauskaitė, A. Menteş, Production of magnetically recoverable, thermally stable, bio-based catalyst: Remarkable turnover frequency and reusability in Suzuki coupling reaction, Chem. Eng. J. 331 (2018) 102–113.